AIAA AVIATION Forum
17-21 June 2019, Dallas, Texas
AIAA Aviation 2019 Forum

10.2514/6.2019-3622

Flight Profile Optimization for Noise Abatement and Fuel Efficiency during Departure and Arrival of an Aircraft

Dajung Kim,* Yuan Lyu,† and Rhea P. Liem.‡
The Hong Kong University of Science and Technology, Clear Water Bay, Hong Kong

This paper aims to generate a vertical flight profile that minimizes the perceived aircraft noise around an airport and total fuel consumption over a flight range. Flight profile for an aircraft and fuel consumption are computed from a set of force equilibrium equations for takeoff, climb, cruise, descent, and landing segments and a residual equation. The noise level is estimated using the Nose-Power-Distance metrics of integrated noise model. The aircraft noise level and fuel consumption are optimized concerning varying positions of the vertices of accelerated climb segment and decelerated descent segment by using non-dominated sorting genetic algorithm II. The method will be applied to Boeing 777-300ER flying from Hong Kong International Airport (HKIA) to London Heathrow Airport (LHR) and verified with brute force results.

I. Nomenclature

D	=	drag force
$Fuel^*$	=	optimum fuel consumption
$\overline{Fuel^*}$	=	normalized optimum fuel consumption
$Fuel_{climb,descent}$	=	fuel consumption for climb and descent segment
$Fuel_{cruise}$	=	fuel consumption for cruise segment
$Fuel_{min}$	=	minimum fuel consumption
$Fuel_{max}$	=	maximum fuel consumption
$Fuel_{obj}$	=	objective function for fuel consumption
$Fuel_{takeoff,landing}$	=	objective function for fuel consumption
L	=	lift force
M	=	Mach number
$P_1(x, y)$	=	vertex position between accelerated climb segment and constant velocity climb segment
$P_2(x, y)$	=	vertex position between constant velocity descent segment decelerated descent segment
R	=	flight range
R^*	=	required flight range
RC	=	rate of climb
SEL^*	=	optimum noise level
$\overline{SEL^*}$	=	normalized optimum noise level
$SEL_{T,d}$	=	noise level at engine power T and distance d (dB)
SEL_{min}	=	minimum noise level
SEL_{max}	=	maximum noise level
SEL_{obj}	=	objective function for noise level
T	=	thrust
T_1, T_2	=	engine power values for which noise data are available in the NPD database
$TSFC$	=	thrust specific fuel consumption
V	=	velocity
V_{CAS}	=	calibrated airspeed (knots)
V_{TAS}	=	true airspeed (knots)
V_f	=	final velocity

*Ph.D. Candidate, Department of Mechanical and Aerospace Engineering.
†Ph.D. Candidate, Department of Mechanical and Aerospace Engineering.
‡Assistant Professor, Department of Mechanical and Aerospace Engineering, Member of AIAA.

V_i	=	initial velocity
W	=	weight
W_{TOW}	=	takeoff weight
W_{ZFW}	=	zero fuel weight
W_f	=	final weight
W_i	=	initial weight
d	=	distance
d_1, d_2	=	distance values for which noise data are available in the NPD database
f_{obj}	=	objective function
g	=	gravitational acceleration
h	=	altitude
h_f	=	final altitude
h_i	=	initial altitude
t	=	time
t_f	=	final time
t_i	=	initial time
y_1, y_2	=	altitude of $P_1(x, y)$ and $P_2(x, y)$
y_{max}	=	maximum altitude of $P_1(x, y)$ and $P_2(x, y)$
y_{min}	=	minimum altitude of $P_1(x, y)$ and $P_2(x, y)$
γ_{climb}	=	climb angle of accelerated climb segment
$\gamma_{descent}$	=	descent angle of decelerated descent segment
δ	=	pressure ratio at aircraft altitude
θ	=	temperature ratio at aircraft altitude
μ_r	=	coefficient of the rolling friction
σ	=	air density ratio at aircraft altitude
ω	=	weighting parameter

II. Introduction

Efforts to reduce airplane noise have increased as air traffic volume has increased rapidly over the past decade and the aircraft noise has had a negative impact on the health of residents around the airport. There are three main methods to reduce aircraft noise: 1) To change the design to eliminate the noise source itself, 2) to reduce the number of aircraft arriving and departing at the same time through flight arrival/departure schedules, 3) to modify the profile when departing or arriving at the airport. Since the change of the profile of arrival and departure can be easily applied, compared to the other options, researches in this field are increasing recently.

Heinz et al. [1] proposed a technique for calculating optimum profile for noise abatement by introducing two mathematically defined criteria as a basis and dynamic programming. Although the optimization method used in this study has the simplicity of inequality constraints on the state variable, such as airspeed and altitude, it is computationally inefficient. Moreover, noise prediction has low-fidelity. S Hartjes et al. [2] and Hogenhuis et al. [3] explored noise-optimized departure and arrivals around Amsterdam Airport Schiphol using the direct optimization technique of collocation with non-linear programming. Gradient-based methods can only be applied to models that can be expressed in terms of a smooth differentiable function and noise model used in this study, although it derived from INM, only considers a specific aircraft type. Xavier et al. [4] applied a lexicographic multi-objective optimization techniques in an effort to minimize the aircraft noise impact modeled by using fuzzy logic in a hospital, a school, two residential zones, and an industrial zone. However, the noise model used in this study cannot represent different aircraft types and different departures (different final points) corresponding to a realistic scenario of an existing airport with its surrounding features. Ho Huu Vinh et al. [5] used a multi-objective evolutionary algorithm based on decomposition to design departure flight profiles for noise abatement predicted by Integrated Noise Model (INM), and compared with an elitist non-dominated sorting genetic algorithm. Decomposing multi-objective optimization problems into a number of scalar optimization sub-problems in this study leads to a significant reduction in the number of model evaluations and runtime typically required for an evolutionary algorithm. However, an evolutionary algorithm does not always guarantee a global optimal solution.

The proposed algorithm aims to generate optimal aircraft flight profiles with respect to the perceived noise level around an airport and total fuel consumption along the flight profile. Noise-Power-Distance metrics of INM model is

applied for noise model and a set of for equilibrium equations and its residual equation are computed to obtain fuel consumption and flight profile. Optimization method used in this study is the Non dominated sorting genetic algorithm II (NSGA-II) considering the nature of objective functions. To illustrate the capability of the proposed algorithm, an example scenario, Boeing 777-300ER departing from Hong Kong International Airport (HKIA) and landing at London Heathrow Airport (LHR), is set.

III. Optimization problem description

In this work, we investigate optimum flight profiles which can reduce perceived noise level on the ground and total fuel consumption of an aircraft by changing the positions of the end point of the accelerated climb and the starting point of the decelerated descent. Table 1 summarizes optimization problem we study in this paper.

Table 1 Optimization problem formulation

	Function/variable	Description
minimize	SEL_{obj}	Aircraft noise level
	$Fuel_{obj}$	Fuel consumption
with respect to	$P_1(x, y)$	Climb vertex position
	$P_2(x, y)$	Descent vertex position
subject to	$\gamma_{climb} \leq \gamma_{max}$	Climb angle
	$\gamma_{descent} \leq \gamma_{max}$	Descent angle
	$R = R^*$	Flight range
	$y_{min} \leq y_1 \leq y_{max}$	Altitude of $P_1(x, y)$
	$y_{min} \leq y_2 \leq y_{max}$	Altitude of $P_2(x, y)$

We seek to minimize the noise level and fuel consumption over a broad set of flight profiles which has less than 15-degree climb and approach angle and can meet the flight range requirement by solving a set of motion equilibrium equations. As shown in Fig. 1, the proposed optimization framework calculates flight profile varying with the change of vertex positions of each flight profile segment. Perturbing the positions of two vertex points can change the distance between an aircraft and an observer on the ground, and thus improve the noise level. It also can generate the whole flight trajectory which is highly related to fuel consumption.

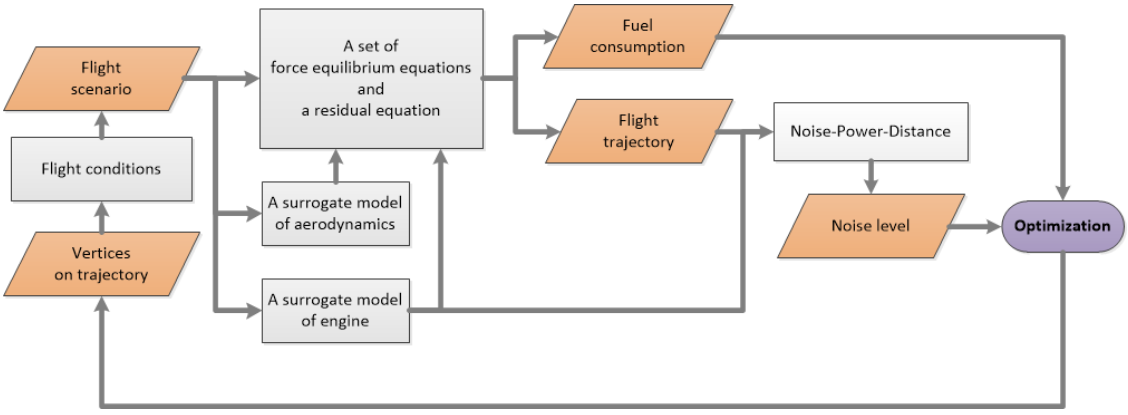

Fig. 1 Flowchart of the noise and fuel consumption minimization problem

For example, if the altitude of the end point of accelerated climb segment becomes higher with the same velocity condition at that point, the perceived noise level on the ground could be smaller. However, the engine will consume more fuel to reach that point with the same speed condition as the one with lower altitude. The perceived noise level on the ground and the fuel consumption are conflicting under this assumption. Fig. 2 shows the solution surface of fuel

consumption, noise level, and summation of fuel consumption and noise level. As these solution surfaces are illustrated, the optimization problem is a non-linear and non-smooth multi-objective problem.

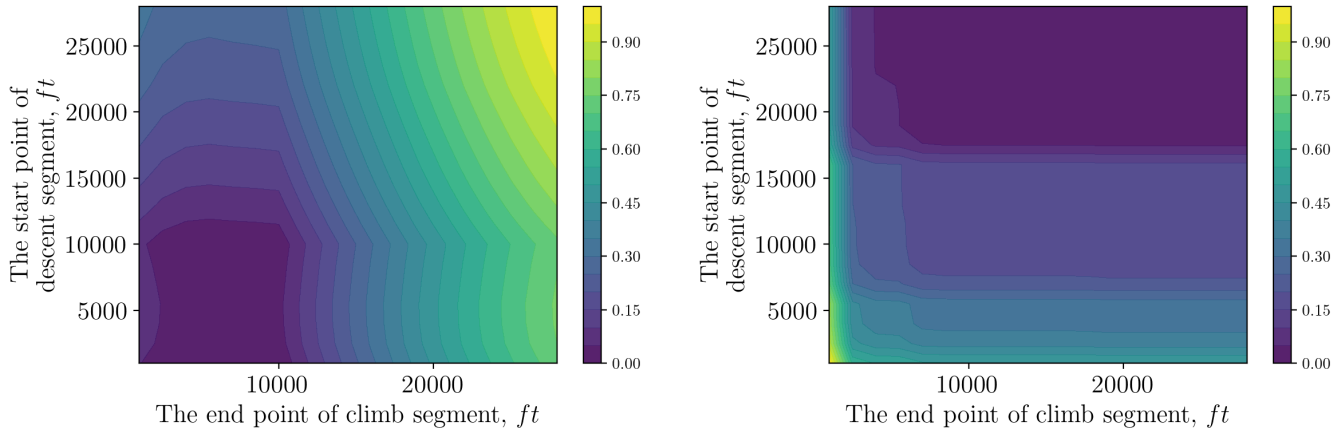

(a) Fuel consumption **(b) Noise level**

Fig. 2 Solution surface

A. Objective function

In this section, we describe the physical model of two objective functions, noise level, and fuel consumption.

1. Noise level

The noise prediction model used in this study is the Noise-Power-Distance (NPD) metrics from the Integrated Noise Model (INM) [6] of the Federal Aviation Administration (FAA). As shown in Fig. 3, the NPD metrics can estimate A-weighted sound exposure level based on aircraft types, the engine power of the aircraft according to the operating modes, such as departure or approach, and the distance between the observer and the aircraft.

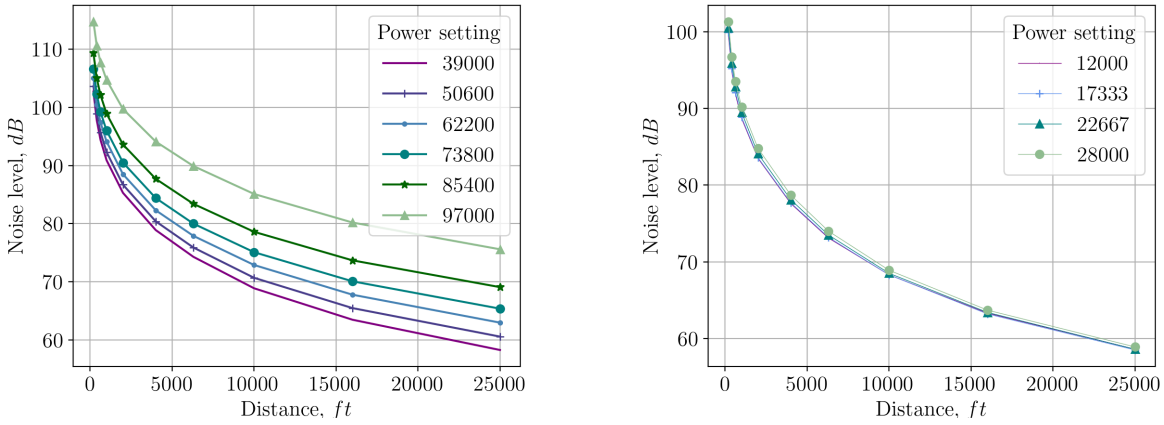

(a) Departure **(b) Arrival**

Fig. 3 The Noise-Power-Distance [7]

To obtain noise levels that lie between thrust values, between distance values or outside of the bounding thrust or distances values, linear interpolation/extrapolation on thrust and logarithmic interpolation/extrapolation on distance are used. The distance interpolation/extrapolation of the noise level in decibels at thrust, P_1 is shown as

$$SEL_{T_1,d} = SEL_{T_1,d_1} + \frac{(SEL_{T_1,d_2} - SEL_{T_1,d_1}) \cdot (\log_{10} d - \log_{10} d_1)}{(\log_{10} d_2 - \log_{10} d_1)}. \quad (1)$$

The engine power interpolation/extrapolation of the noise level in decibels at thrust P and distance d is given as

$$SEL_{T,d} = SEL_{T_1,d} + \frac{(SEL_{T_2,d} - SEL_{T_1,d}) \cdot (T - T_1)}{(T_2 - T_1)}. \quad (2)$$

The distance between an observer and an airplane is a Euclidean distance. In order to well reflect the perceived noise on the ground, we used the observer's position varies with flight segments. The observer is assumed to be located at the starting point of takeoff ground roll and at the ending point of landing ground roll for takeoff and landing stage respectively. However, the observer is moving with aircraft during climb and descent stages so the observer on the ground is always right below the aircraft.

The thrust of the aircraft is predicted using a surrogate model of B777 engine. The surrogate models will compute engine thrust and specific fuel consumption according to altitude, throttle, velocity input using the Regularized Minimal-energy Tensor product B-splines (RMTB) [8] of the Surrogate Modeling Toolbox developed by the Department of Aerospace Engineering at Michigan, NASA, ISAE-SUPAERO, and the ONERA French Aerospace Laboratory [9].

Accumulated sound exposure levels from the starting point of takeoff ground roll to the end of accelerated climb segment and from the starting point of the decelerated descent segment to the end of the landing ground roll are estimated as

$$SEL_{obj} = 10 \cdot \log_{10} \sum_{j=1}^{n} SEL_{seg=j}(P(x_{Aircraft}, y_{Aircraft}), P(x_{observer}, y_{observer}), T, Operating\ mode), \quad (3)$$

and used as one of the objective functions.

2. Fuel consumption

The fuel burn is computed by performing a detailed mission analysis procedure that solves a set of flight equilibrium of each flight segment and its residual equation developed by Liem et al. [10] [11]. Zero fuel weight and flight range are given as the simulation inputs and takeoff weight is assumed and repeatably calculated with the set of the flight equilibrium equations for each flight phase and corresponding fuel consumption [12]. Since the assumed takeoff weight subtracted by fuel consumption should match with the zero fuel weight, we obtain fuel consumption of each segment and of each interval which consists of a segment through this iterative procedure using the Newton–Krylov algorithm. Eq. (4) denotes that weight at the vertex points of two adjacent segments should be matched,

$$W_{f_{j+1}} = W_{i_j}, \quad (4)$$

where j=1,...,N_{seg} is the segment index, and subscripts i and f are for initial and final, respectively. Eq. (5) describes that the initial weight of the first segment should be equal to the takeoff weight, W_{TOW}, and that final weight of the last segment should be the same as the zero fuel weight such as

$$W_{i_1} = W_{TOW} \text{ and } W_{f_{seg}} = W_{ZFW}. \quad (5)$$

Flight segments are typically comprised of five different types of segments, takeoff, climb, cruise, descent, and landing as shown in Fig. 4. Each of the segments is analyzed independently by employing a force equilibrium equation considering the physics of each segment.

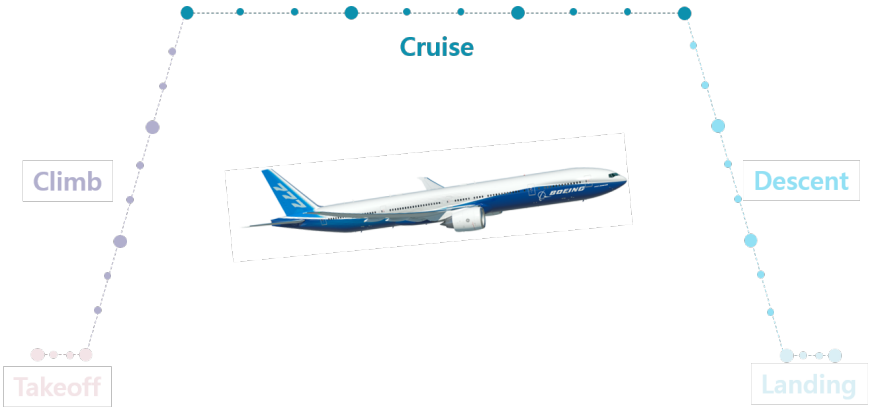

Fig. 4 Typical flight profile

Fuel consumption equations of takeoff and landing, climb and descent, and cruise can be denoted as

$$
\begin{aligned}
Fuel_{takeoff,landing} &= \int_{V_i}^{V_f} -TSFC \cdot T \frac{W}{g[T - D - \mu_r(W - L)]} dV, \\
Fuel_{climb,descent} &= \int_{h_i}^{h_f} \frac{-TSFC \cdot T}{RC} dh, \\
Fuel_{cruise} &= \int_{t_i}^{tf} -TSFC \cdot T dt.
\end{aligned} \tag{6}
$$

where V is the velocity given as an input. Thrust specific fuel consumption $TSFC$ and thrust T are computed using a surrogate model of an engine described in noise level part. A surrogate model of aerodynamics to estimate drag D, and lift L with the input of the flight conditions such as the angle of attack and velocity. 35 sample points for the training data of the surrogate model are selected by Halton sequences and drag and lift coefficient are computed with Raynolds-Averaged Navier-Stokes (RANS) simulations using SU2 [13]. The aerodynamics surrogate model is also implemented by using the RMTB model as the engine surrogate model and validated by the wind tunnel test data of NASA common research model [14].

Total fuel consumption along a flight profile is the arithmetic sum of fuel consumption of each segment given as

$$
Fuel_{obj} = \sum_{j=1}^{n} Fuel_{seg=j}. \tag{7}
$$

B. Design variables

We consider two variables, which are the end point of the accelerated climb segment and the starting point of the decelerated descent segment as control points of the profile. Fig. 5 shows the positions of those two control points over the whole flight range. Since the aircraft at low altitude has a significant effect on the total noise level perceived on the ground, changing climb and descent angles are considered as the most critical to the noise near an urban area. Although fuel consumption mostly depends on the flight range or the weather condition rather than the climb or descent angle, flight condition of acceleration and deceleration parts have an impact on total fuel consumption. Therefore two variable that lies on the vertex of the accelerated climb and constant velocity climb, and constant velocity descent and decelerated descent are chosen to design variable of the optimization problem.

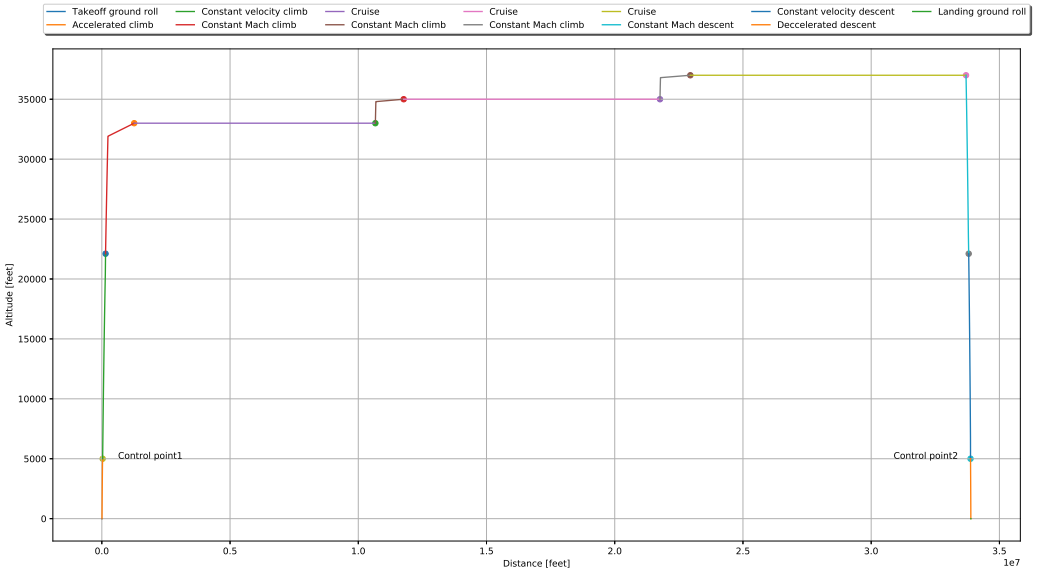

Fig. 5 Variables (control points) of objective functions

C. Constraints

There are five constraints in this problem: a climb angle, a descent angle, a flight range, the altitude of the end point of accelerated climb segment, and the altitude of the start point of decelerated descent segment. In case of the climb angle and the descent angle, we set maximum values of these angles as 15 degrees. Considering the fact that the average maximum climb angle of the actual flights is around 7 degrees to 8 degrees, the setting values of the maximum climb and descent angle can expand the variation range of the design variables while maintaining the physics theory consistently as shown in Fig. 6. The flight range is one of the constraints of this optimization problem as well as the input variables of the iteration process in the fuel consumption estimation and flight profile generation. The details of flight range are described in section IV C. The altitude variation range of the end point of accelerated climb segment and the start point of decelerated descent segment are both from 1,000 feet to 27,000 feet, reflecting the range of the climb and descent angle.

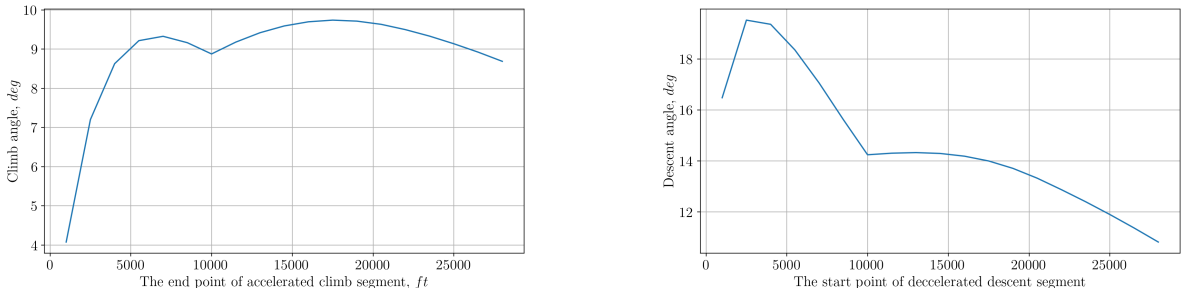

(a) Climb angle **(b) Approach angle**

Fig. 6 Angles with respect to control points

D. Optimization algorithm

Mathematically, a single global solution to a multiobjective problem does not exist unless the utopia point happens to be attainable. However, we can get either a set of optimum solution or an optimum solution by assuming the preferences,

a decision maker's opinions concerning points in the feasible solution space. Two methods categorized by the way to set preferences are used in this study. One is a posteriori method which gives the representative subset of Pareto optimum solution and the other is a priori method which entails one optimum solution with specified preferences by scalarizing two objective functions to a single objective function [15].

1. A posteriori method

To obtain a set optimum solution between two objective functions, noise level, and fuel consumption, we choose the Non-dominated Sorting Genetic Algorithm II (NSGA-II) [16]. As previously mentioned, the optimization problem we set in this study is a non-linear and non-smooth multi-objective problem. In this case, mathematical approaches can easily fail to give a global solution. The NSGA-II is one of the most potent meta-heuristic algorithms which can be valid regardless of the nature of the objective functions and constraints. Algorithm 1 shows pseudocode of the NSGA-II. It evaluates and improves a group of potential solutions with randomly generated variables by sorting them based on their ranks and the crowding distances. The optimization framework is implemented using the pyOpt module [17].

Result: Subset of Pareto frontier(P)
Initialization P and P';
for $p \in P'$ *and* $p \notin P$ **do**
  Add p to P temporarily;
  if p *dominates* $q \in P$ **then**
    Delete q from P;
  else
    Delete p from P;
  end
  Sort the elements of P with respect to its rank and crowding distance;
end

Algorithm 1: The Non-dominated Sorting Genetic Algorithm II (NSGA-II)

Since the noise level is in a logarithmic scale and has minimum variations compared to the fuel consumption, the two objective functions (noise level and fuel consumption) are normalized as

$$\begin{aligned} \overline{Fuel^*} &= \frac{Fuel^* - Fuel_{min}}{Fuel_{max} - Fuel_{min}}, \\ \overline{SEL^*} &= \frac{SEL^* - SEL_{min}}{SEL_{max} - SEL_{min}}. \end{aligned} \tag{8}$$

$Fuel^*$ and L^* in Eq. (8) have values between zero to one, depending on the accuracy of the predicted value of their maximum and minimum [18].

2. A priori method

A priori method formulates a single-objective optimization problem by specifying preferences which may be articulated in terms of the importance of each objective, reflecting decision-maker's preferences. The weighted sum method, one of the most common scalarization methods for multi-objective optimization, is used in this study, and is shown as

$$f_{obj} = \omega \cdot \overline{Fuel^*} + (1 - \omega) \cdot \overline{SEL^*}. \tag{9}$$

ω are the user-specified weights less than or equal to one. In order to consider the effect of noise level and fuel consumption equally, we set $\omega = 0.5$ in this study.

IV. Flight simulation

This section describes the simulation setup for applying the optimization problem established in section III. We first present the baseline aircraft, followed by a simulation scenario derived from actual flight data. We then discuss the overall procedure for performing the optimization.

A. Aircraft type

An aircraft type used through this research is Boeing 777-300ER with two GE90 engines. Detailed specifications are shown in the Table 2.

Table 2 The specifications of Boeing 777-300ER

Parameter	Value	Units
Wing span reference	212.6	ft
Wing sweep	31.6	deg
Wing reference area	4,701.7	ft^2
Maximum takeoff weight	774,924.8	lb
Operating empty weight	369,935.7	lb
Maximum landing weight	553,999.6	lb
Thrust(x2) GE	ll5102.2	lbf

B. Simulation scenario

A flight scenario departing from Hong Kong International Airport (HKIA) and landing at London Heathrow Airport (LHR) is chosen as a simulation scenario in this study. Six actual flight trajectories presented in Fig. 7 are examined to create a simulation scenario. Considering these trajectories, cruise altitude is set to be 33,000, 35,000, and 37,000 as shown in Table 3. Total of 13 segments within a flight are assigned, and each segment has ten intervals. Control points lie on the vertex between the second segment and the third segment and the vertex between eleventh and twelfth segment in Table 3.

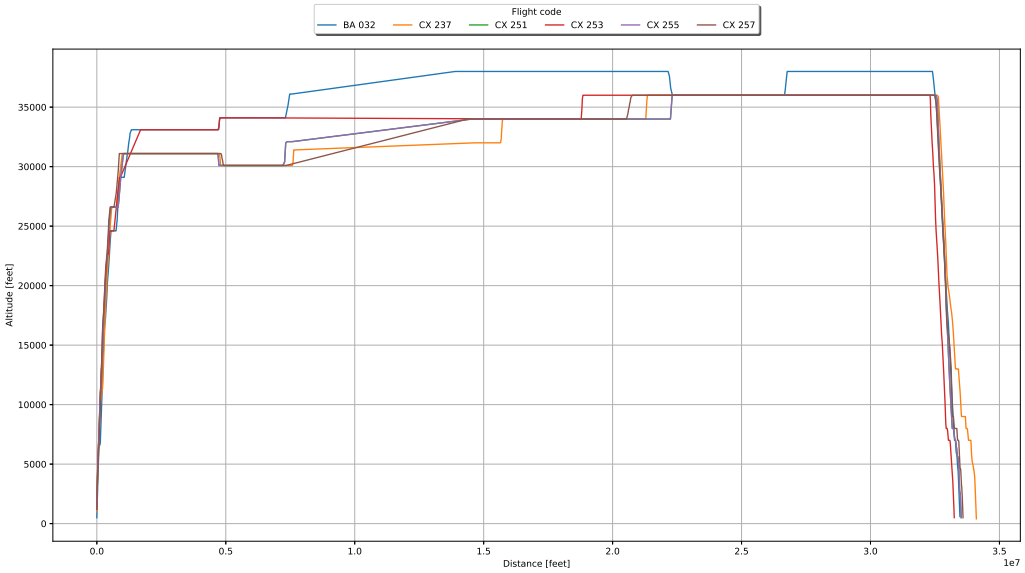

Fig. 7 Actual flight trajectories from Hong Kong to London

Table 3 Input parameters of the simulation

	Segment	Altitude [ft]	Speed
1	Takeoff	0 → 0	0 → 150 KIAS
2	Climb	0 → Control point1	150 KAIS → Control point1
3	Climb	Control point1 → 29,180	Control point1 → 310 KIAS
4	Climb	29,180 → 33,000	M 0.82
5	Cruise	33,000	M 0.82
6	Climb	33,000 → 35,000	M 0.82
7	Cruise	35,000	M 0.82
8	Climb	35,000 → 37,000	M 0.82
9	Cruise	37,000	M 0.82
10	Descent	37,000 → 29,180	M 0.82
11	Descent	29,180 → Control point2	310 KIAS → Control point2
12	Descent	Control point2 → 0	Control point2 → 150 KIAS
13	Landing	0 → 0	150 KIAS → 0
	Total flight range		3.37047e7 [feet]
	Zero fuel weight		500,722 [lb]

C. Simulation input

The average value of zero fuel weight in Fig. 8 a), flight range in Fig. 8 b) and cruise speed in Fig. 8 c) of total 1,750 aircraft departing from HKIA to LHR from January to December 2017 was used as the simulation input value [19]. Table 3 presents detailed information about simulation input. After generating the flight profile with the given input values, the fuel consumption model was verified by comparing the predicted fuel consumption with the average value of the actual data, as shown in Fig. 8 d). The altitude of the two control points are set to be 7,500 feet, and the fuel consumption calculated in this simulation is 217652.2 pounds which have 0.2 percent of relative error compared to the average value of fuel consumption in actual flights.

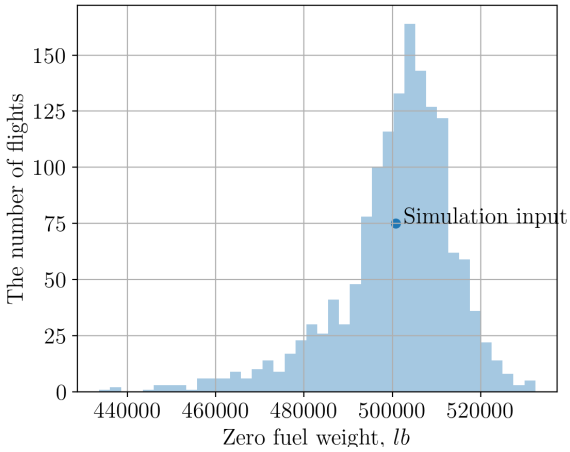

(a) Zero fuel weight

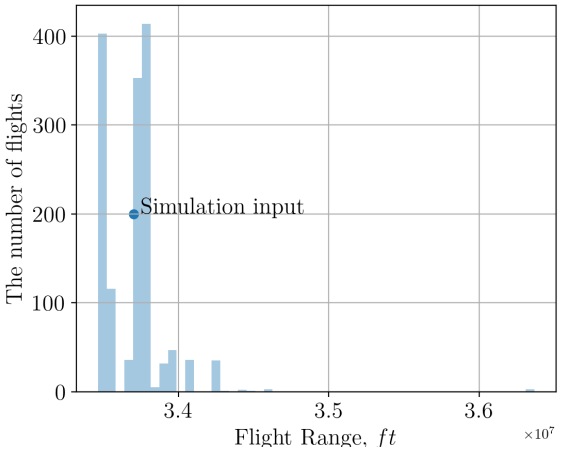

(b) Flight range

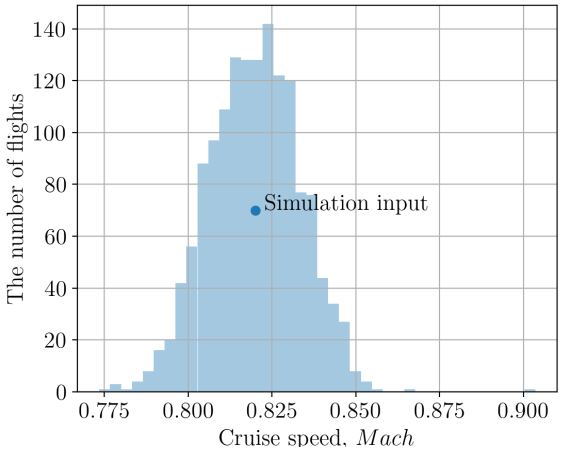

(c) Cruise speed

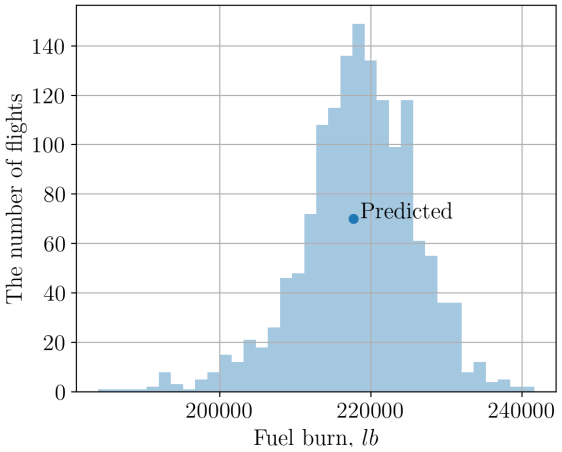

(d) Fuel consumption

Fig. 8 Distribution of the actual flight data

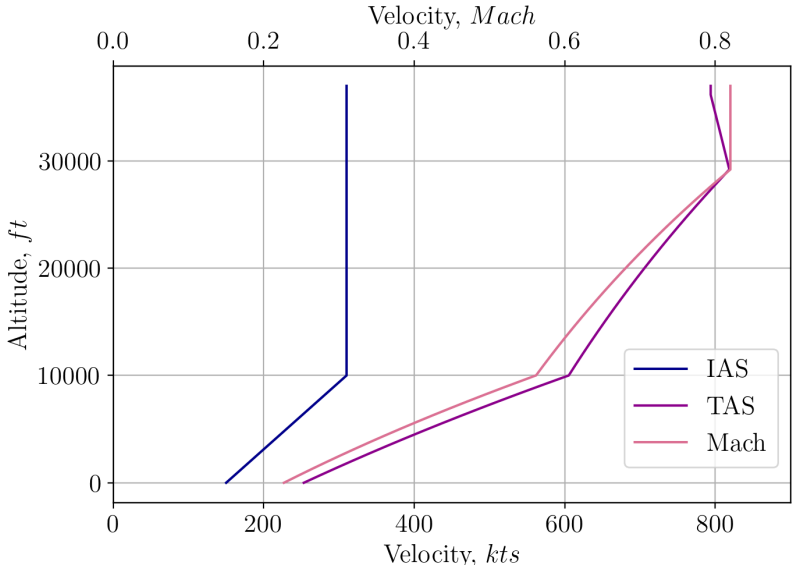

Fig. 9 Velocity profile for the simulation

Fig. 9 shows a velocity profile of the simulation. Indicated Air Speed (IAS) is assumed to be the same as Calibrated Air Speed (CAS) and converted into True Air Speed (TAS) by applying Eq. 10 shown as,

$$V_{TAS} = V_{CAS} \cdot \sigma^{-1/2}$$
$$\sigma = \frac{\delta}{\theta} = \left[1 - \left(\frac{0.003566 \cdot h}{518.67}\right)\right]^{4.256}, \tag{10}$$

when airport pressure is 29.92 inches of mercury relative to mean sea level, airport temperature is 59 ^{o}F, and the airport elevation is 0 feet mean sea level [20]. IAS linearly increases from 256 knots to 310 knots as altitude increases from 0 feet to 10,000 feet. IAS is set to be a constant as 310 knots above altitude 10,000 feet, but TAS is varying with altitude because of the density ratio change along with altitude change. When the corresponding Mach number reaches to 0.82, the airplane keeps this Mach number constantly before it descends and passes the same altitude which it starts to maintain the constant Mach number 0.82 at [10].

V. Results and Discussion

In this section, we present the results of noise reduction and fuel efficient optimization for B777-300ER departing from HKIA and landing at LHR.

A. A posteriori method

We validate the optimization results with feasible area calculated by a brute force approach. Fig. 10 is feasible area obtained from a brute force approach. We divide the altitude from 1,000 feet to 20,000 feet by 1,000 and for both departing and arriving. By varying this altitude of control points, a total of 400 combinations of the case are created. Each of the cases generates a different route based on the force balance of flight segments, and it also calculates total fuel consumption and noise level around the airport. Those fuel consumption and noise level are normalized and plotted in Fig. 10. Feasible area means the points which satisfy the constraints. Triangle marks on Fig. 10 denote the Pareto frontier of this optimization problem. Fig. 11 is the optimization results of a posteriori method. The population size we set here is 52, so 52 points of the Pareto frontier of the optimization problem obtained successfully compared with Fig. 10.

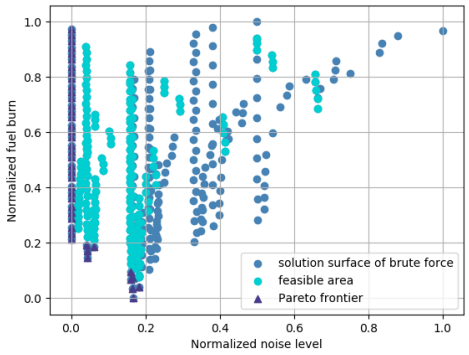

Fig. 10 Brute force approach

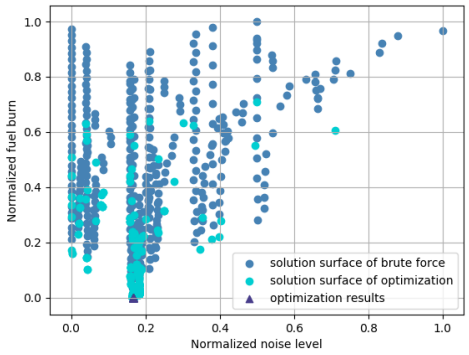

Fig. 11 Results of posteriori optimization

As we can see in Fig. 12, the initial population evolved into the final optimum population, which can obtain less fuel consumption through 100 generations. However, it seems that the number of mutation is not sufficient to find the optimum points in terms of the noise level. In Fig. 13 and Fig. 13, we compared the optimization results with the actual data used for simulation setup and mentioned in section IV. The noise level has been reduced by 1.5 dB, and Fuel consumption also has been decreased by 159.8 pounds. The optimum vertical flight profile of a flight departing and landing are shown in Figs. 15 and 16.

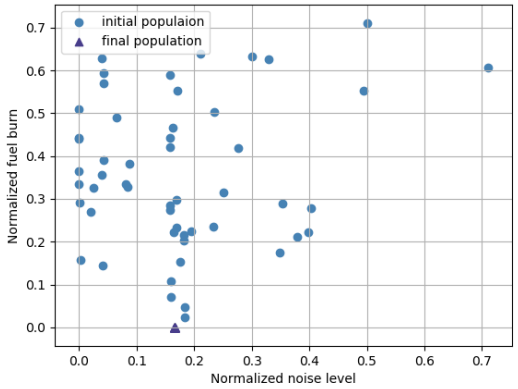

Fig. 12 Initial and final results of posteriori optimization

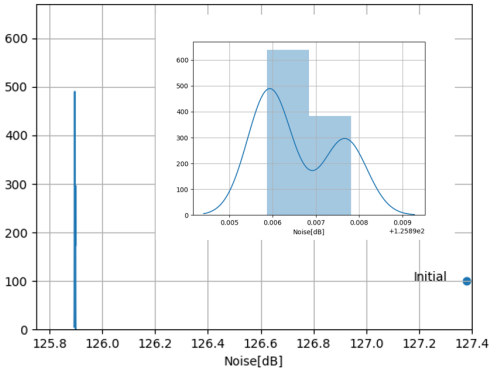

Fig. 13 Noise reduction

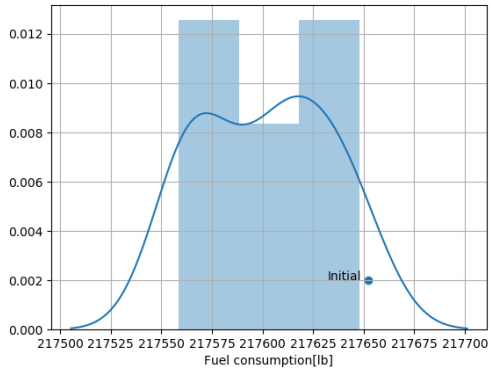

Fig. 14 Fuel reduction

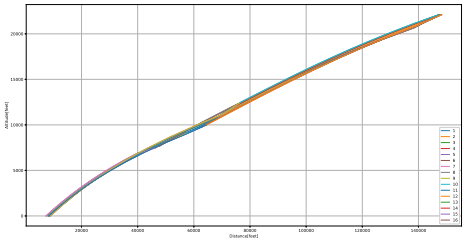

Fig. 15 Optimum departure routes

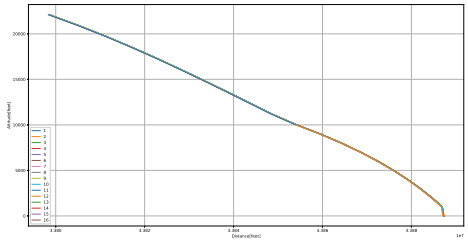

Fig. 16 Optimum arrival routes

B. A priori method

One set of optimum control points was found considering noise level and fuel consumption in the same ratio. The endpoint of the accelerated climb segment is 9999.2 feet, and the start point of the decelerated descent segment is 10000.0 feet. Based on these control points, we found an optimum flight path concerning noise level near the airports and total fuel consumption, as shown in Fig. 17. The total fuel consumption in the optimum route is 217,558.5 pounds. The noise near the airport at the departure is 150.9 dB, and the noise near the airport at the arrival is 100.9 dB. Therefore, noise reduction compared to the baseline route is 1.5 dB, and the fuel consumption decreased by 93.7 pounds.

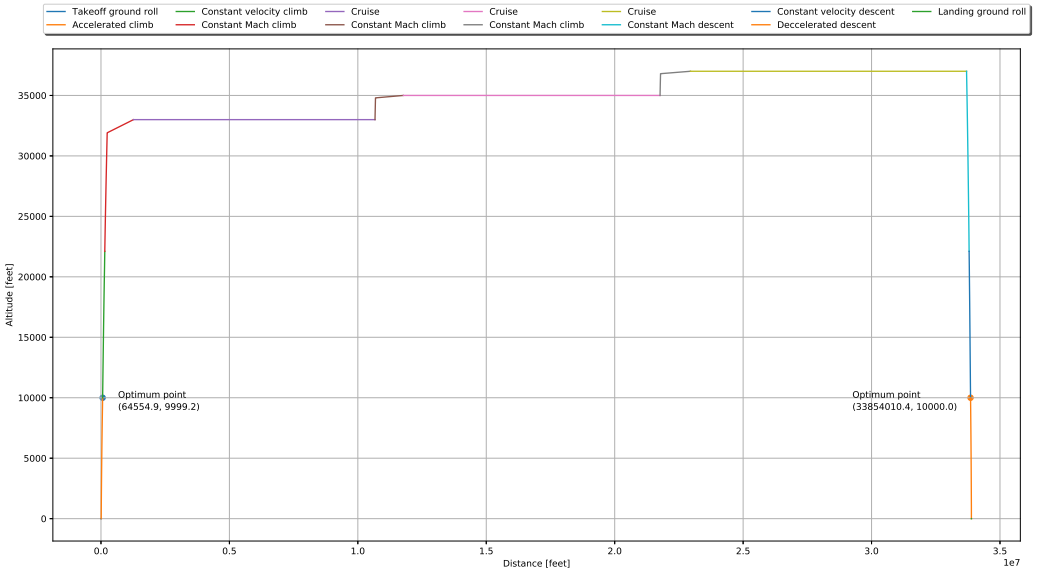

Fig. 17 Optimum route

The change in the scalarized and normalized objective function during the iteration inside of priori optimization process is shown in Fig. 18. As the number of iteration increases, the value of the normalized objective function decreases. Although the maximum number of iterations which is set to 50 seems too large in this case, it is necessary to perform an additional convergence test to determine the appropriate number of iteration since the convergence speed varies depending on the initial value setting.

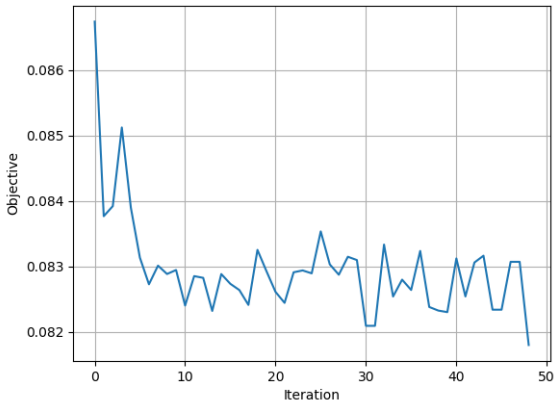

Fig. 18 Convergence

Fig. 19 and Fig. 20 show zoomed departing and arriving flight routes, respectively. Flight paths with a similar climb and descent angles are generated to compare fuel consumption because there is no fuel consumption information for a given actual path. The calculated fuel consumption is compared with the amount of fuel consumed in the optimized path. The total fuel consumption can be reduced by 322.3 pounds. In the case of the noise level, the noise level on a departing flight profile can be decreased by 0.01 dB, and the noise level on arriving flight profile is rather increased by 9.9 dB. When the actual landing, the approach angle is very small, and the starting point of deceleration comes earlier than the one in the simulation result. Therefore, optimization should be performed with smaller constraint angle than 15 degrees.

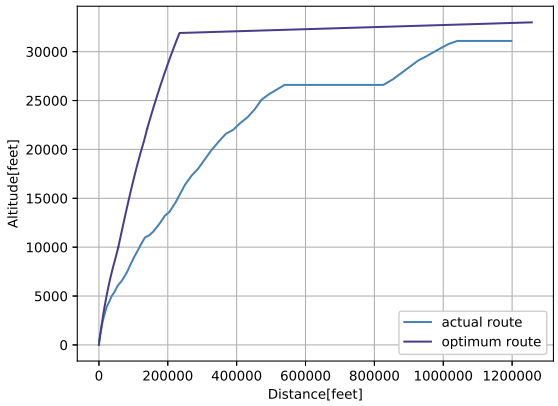

Fig. 19 Departing flight profile from HKIA

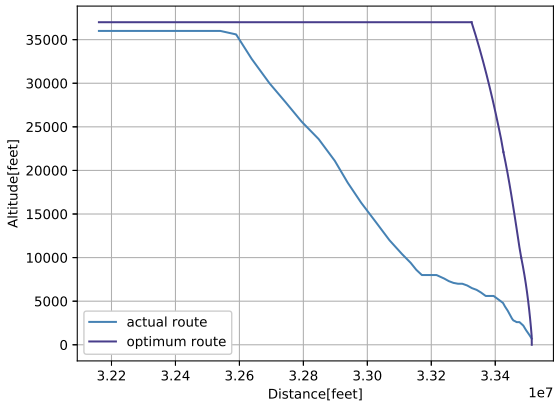

Fig. 20 Arriving flight profile at LHR

The climb and descent angle of the optimal path is more significant than the actual path. However, the climb angle and the descent angle according to the flight range during a flight along the optimum route is shown in Fig. 21, and they do not exceed the limit angle of 15 degrees.

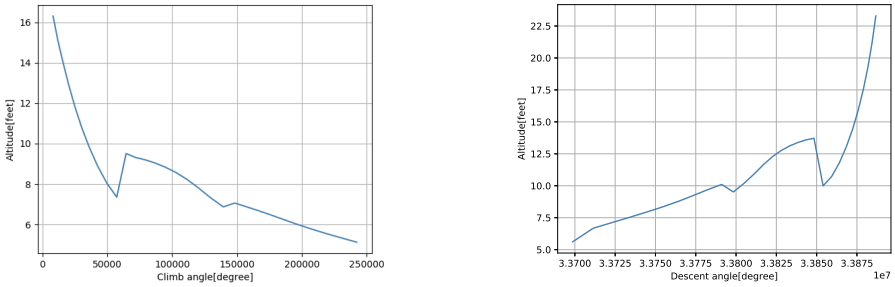

Fig. 21 a)Climb angle b)Descent angle along a optimum flight range

VI. Conclusion

A new method for performing aircraft noise level and fuel consumption optimization varying flight routes has been presented. The point of difference in this study is the presented method can easily find the optimum path that depends on the zero fuel weight, considering noise signature on the ground and total fuel consumption during a flight simultaneously. The noise model herein estimates aircraft noise level perceived by an observer moving on the ground along a flight path of an airplane in a short time. The path generation algorithm applied in this study can provide positions and flight conditions of each flight path relatively quickly by segmenting it as 13 segments. It also can predict high fidelity fuel consumption values for each segment. Combining these two models with optimization procedure allows us to get the flight path which has optimum noise level and fuel consumption within the flight range and for specific zero fuel weight with computationally low cost. Although it is only applicable for vertical flight profile, the results will still provide the operational direction of an airplane according to the altitude change.

Analysis of 1,750 historical flights data is performed to reflect actual flight cases into the optimization simulation. RANS simulation is conducted for 35 sample points of aerodynamics surrogate model. Brute force simulation for 400 combinations of two control points is carried out to be compared with the results from the optimization framework

The method is demonstrated in the profile optimization of B777-300ER flying from Hong Kong to London. The optimization results of a posteriori method are compared with base simulation results. The average noise level is reduced by 1.5 dB, and the fuel consumption is decreased by 159.8 pounds. The optimization results of a priori method are also compared with the base simulation results as well as the simulation based on the actual flight profile. In the case of the comparison between base simulation, the noise level is declined by 1.5 dB and the fuel consumption is decreased by 93.7 pounds. However, when it comes to the comparison between an actual flight profile, although the fuel consumption is reduced by 322.3 pounds, the arriving noise level around an airport is increased by 9.9 dB because of the steep descent angle. Hence, more strict angle constraint is needed to be applied.

In this study, the accelerated climb segment and decelerated descent segment were designated as one flight segment respectively. Since the type of the flight path segments must be set as input to the path generation and fuel consumption calculation algorithms, optimization should be done with control points only at the ends of the flight segment, so the optimization was performed only for the continuous climb and continuous descent. In the Future, we will assign accelerated climb segment and decelerated descent segment as several segments and then the optimization will be performed for a step climb and step descent. The noise level and fuel consumption optimization results of a step climb and descent will be compared with the results of continuous climb and descent.

Acknowledgments

The work was supported by the Hong Kong Research Grant Council Early Career Scheme (Project No. 26202116).

References

[1] Erzberger, H., and Lee, H. Q., "Technique for calculating optimal takeoff and climbout trajectories for noise abatement," 1969.

[2] Hartjes, S., Visser, H., and Hebly, S., "Optimisation of RNAV noise and emission abatement standard instrument departures," *The Aeronautical Journal*, Vol. 114, No. 1162, 2010, pp. 757–767. doi:10.1017/S0001924000004243.

[3] Hogenhuis, R., Hebly, S., and Visser, H., "Optimization of area navigation noise abatement approach trajectories," *Proceedings of the Institution of Mechanical Engineers, Part G: Journal of Aerospace Engineering*, Vol. 225, No. 5, 2011, pp. 513–521. doi:10.1177/09544100JAERO840.

[4] Prats, X., Puig, V., Quevedo, J., and Nejjari, F., "Multi-objective optimisation for aircraft departure trajectories minimising noise annoyance," *Transportation Research Part C: Emerging Technologies*, Vol. 18, No. 6, 2010, pp. 975–989. doi: 10.1016/j.trc.2010.03.001.

[5] Ho-Huu, V., Hartjes, S., Geijselaers, L., Visser, H., and Curran, R., "Optimization of noise abatement aircraft terminal routes using a multi-objective evolutionary algorithm based on decomposition," 2017. doi:10.1016/j.trpro.2018.02.014.

[6] SAE (ed.), *Procedure for the Calculation of Airplane Noise in the Vicinity of Airports*, AIRl845, 1845.

[7] Organization, I. C. A. (ed.), *Environmental protection, aircraft noise*, Annex 16, Vol. 1., 2008.

[8] Hwang, J. T., and Martins, J. R., "A fast-prediction surrogate model for large datasets," *Aerospace Science and Technology*, Vol. 75, 2018, pp. 74–87.

[9] Bouhlel, M. A., T. Hwang, J., Bartoli, N., Lafage, R., Morlier, J., and Martins, J., "A Python surrogate modeling framework with derivatives," *Advances in Engineering Software*, 2019. doi:10.1016/j.advengsoft.2019.03.005.

[10] Liem, R. P., and Martins, J., "Surrogate models and mixtures of experts in aerodynamic performance prediction for mission analysis," *15th AIAA/ISSMO Multidisciplinary Analysis and Optimization Conference*, 2014, p. 2301.

[11] Rhea P Liem, Y. L. (ed.), *Integrated Eco-Friendly Aircraft Design Framework for a Low-Emission and Low-Noise Aircraft*, Mid-term Progress Report 26202116, 2018.

[12] Liem, R. P. (ed.), *Integrated Eco-Friendly Aircraft Design Framework for a Low-Emission and Low-Noise Aircraft*, Early Career Scheme Proposal 2016/2017, 2016.

[13] Economon, T. D., Palacios, F., Copeland, S. R., Lukaczyk, T. W., and Alonso, J. J., "SU2: An open-source suite for multiphysics simulation and design," *Aiaa Journal*, Vol. 54, No. 3, 2015, pp. 828–846.

[14] "NASA Common Research Model," `https://commonresearchmodel.larc.nasa.gov/experimental-data/`, 2017.

[15] Hwang, C.-L., and Masud, A. S. M., *Multiple objective decision making—methods and applications: a state-of-the-art survey*, Vol. 164, Springer Science & Business Media, 2012.

[16] Deb, K., "A fast elitist non-dominated sorting genetic algorithm for multi-objective optimization: NSGA-2," *IEEE Trans. Evol. Comput.*, Vol. 6, No. 2, 2002, pp. 182–197.

[17] Perez, R. E., Jansen, P. W., and Martins, J. R., "pyOpt: a Python-based object-oriented framework for nonlinear constrained optimization," *Structural and Multidisciplinary Optimization*, Vol. 45, No. 1, 2012, pp. 101–118.

[18] Koski, J., "Multicriterion optimization in structural design," Tech. rep., TAMPERE UNIV OF TECHNOLOGY (FINLAND), 1981.

[19] Yanto, J., and Liem, R. P., "Aircraft fuel burn performance study: A data-enhanced modeling approach," *Transportation Research Part D: Transport and Environment*, Vol. 65, 2018, pp. 574–595.

[20] Administration, T. F. A. (ed.), *Optimization of area navigation noise abatement approach trajectories*, INM Technical Manual, 2008.